High-Resolution NMR in Solids: The CPMAS Experiment

COSTANTINO S. YANNONI

IBM Research Laboratory, San Jose, California 95193

Received August 10, 1981 (Revised Manuscript Received April 1, 1982)

Introduction

From the chemists' viewpoint, high-resolution NMR in solids came of age with the development of cross-polarization magic angle spinning (CPMAS), first experimentally realized by Schaefer and Stejskal.[1] This method, which has its roots in more than two decades of ingenious work in many laboratories, combines pulsed NMR with high-speed sample rotation, and, as shown in Figure 1d, can produce "liquidlike" NMR spectra of a solid material. CPMAS experiments yield ^{13}C spectra of organic solids with line widths as narrow as 2 Hz. The resolution of individual carbon chemical shifts not only makes CPMAS attractive as an analytical technique for solids but also provides a method for obtaining new information about solid-state structure and dynamics on the atomic level.

The purpose of this Account is to describe the magnetic resonance concepts underlying this experiment while providing the background for a companion Account which presents results on a variety of chemically interesting solids using variable-temperature CPMAS capability.[2] The focus will be on ^{13}C spectra of organic solids, although the discussion applies equally well to other spin-$^1/_2$ nuclei which can have weak mutual coupling either by virtue of low natural abundance or a small magnetic moment (e.g., ^{31}P, ^{29}Si, ^{15}N, ^{195}Pt, ^{199}Hg, and Sn and Cd isotopes).[3]

The high resolution achievable in solution NMR spectra is shown in Figure 1e in the proton-decoupled ^{13}C spectrum of 34 mg of a benzil derivative dissolved in $CDCl_3$. The small line widths (<1 Hz) result from complete averaging of anisotropic spin interactions (proton dipolar broadening, carbon chemical shift anisotropy) by the random tumbling of molecules in solution. In solids, where such motion is rare, anisotropic interactions are at most incompletely averaged, and the width of the lines in a solid-state ^{13}C spectrum will be much greater (several kilohertz). Furthermore, sensitivity in these spectra is severely reduced by such large line widths and by the low natural abundance and long relaxation times of ^{13}C nuclear spins. Indeed, when the same conditions are used as for the solution NMR (Figure 1e), no ^{13}C spectrum of 680 mg of solid material is even detectable (Figure 1a). Sensitivity is enormously enhanced by proton–carbon cross polarization,[4] and one obtains, in one-tenth of the time, the broad spectrum shown in Figure 1b, which with strong proton decoupling begins to show some resolved features (Figure 1c). Finally, the addition of magic-angle spinning (MAS)[5] improves the resolution dramatically, and results in a well-resolved spectrum (Figure 1d) for only 34 mg of the solid, comparable in sensitivity to the solution spectrum which was obtained over a much longer time period. The splittings in the solid-state spectrum are induced by crystal packing effects.[6]

In this Account, the resolution and sensitivity problems outlined above, as well as the NMR techniques used to address these problems, are discussed. Relevant concepts in spin diffusion and spin temperature are covered in some detail, and a separate section with a current view of resolution limitations in solid-state ^{13}C CPMAS spectra is included.

Proton Dipolar Broadening

The major source of line width in the ^{13}C spectrum of an organic solid is dipolar broadening by nearby (e.g., bonded) protons. A model for the magnetic dipolar interaction of a ^{13}C nucleus with a proton is shown in Figure 2. The ^{13}C magnetic moment experiences lines of force due to the z component, B_z^H, of a magnetic field generated by the proton magnetic moment. B_z^H will add to or subract from the external field and cause an upfield or downfield shift of the ^{13}C resonance, depending on both the proton spin state and the orientation of the internuclear vector with respect to $\mathbf{B}_0$.[7] The spectrum of a sample of identically oriented, magnetically isolated ^{13}C–^1H pairs is a doublet (Figure 2b), centered around the ^{13}C Larmor frequency with a splitting (in Hz):

$$\Delta\nu_{CH} = \frac{\gamma_C}{\pi}|B_z^H| \tag{1}$$

with

$$B_z^H = \frac{\mu_z^H}{r_{CH}^3}\langle 1 - 3\cos^2\theta\rangle$$

γ_C is the ^{13}C gyromagnetic ratio, related to the magnetic moment by $\mu_C = \gamma_C\hbar/2$, and the geometric factors (r_{CH}, θ) are shown in Figure 2. The angular brackets denote an average over molecular motion. ^{13}C–^1H dipolar splittings can be very large; for example, for a C–H bond parallel to $\mathbf{B}_0$, a doublet splitting of 40 kHz would be

(1) (a) J. Schaefer, E. O. Stejskal, and R. Buchdahl, *Macromolecules*, 8, 291 (1975). The ^{13}C CPMAS experiment was suggested by (b) A. Pines, M. G. Gibby, and J. S. Waugh, *Chem. Phys. Lett.*, 15, 373 (1972).

(2) J. R. Lyerla, C. S. Yannoni, and C. A. Fyfe, *Acc. Chem. Res.*, following paper in this issue.

(3) It is possible to obtain similar spectra for ^1H and ^{19}F by using multiple pulse techniques combined with magic angle spinning as suggested by (a) U. Haeberlen and J. S. Waugh, *Phys. Rev.*, 175, 453 (1968), but this is technically more demanding, and a relatively small number of results have been reported: (b) B. C. Gerstein, R. G. Pembleton, R. C. Wilson, and L. M. Ryan, *J. Chem. Phys.*, 66, 361 (1977); L. M. Ryan, R. E. Taylor, A. J. Paff, and B. C. Gerstein, *ibid.*, 72, 508 (1980); G. Scheler, U. Haubenreisser, and H. Rosenberger, *J. Magn. Reson.*, 44, 134 (1981).

(4) A. Pines, M. G. Gibby, and J. S. Waugh, *J. Chem. Phys.*, 59, 569 (1973).

(5) (a) I. J. Lowe, *Phys. Rev. Lett.*, 2, 285 (1959); (b) E. R. Andrew, *Arch. Sci. (Geneva)*, 12, 103 (1959); (c) E. R. Andrew, *Prog. Nucl. Magn. Reson. Spectrosc.*, 8, 1 (1971).

(6) J. I. Crowley, W. W. Fleming, J. R. Lyerla, and C. S. Yannoni, to be published.

(7) J. S. Waugh, *Ann. N.Y. Acad. Sci.*, 70, 900 (1958).

Costantino S. Yannoni attended Harvard College and received his doctorate from Columbia University in 1967. He is currently a Research Staff Member in the Chemical Dynamics Department at the IBM Research Laboratory in San Jose, CA. He has been developing techniques for obtaining high-resolution NMR spectra of solids and applying these techniques to structural and dynamic studies of organic materials.

0001-4842/82/0115-0201$01.25/0

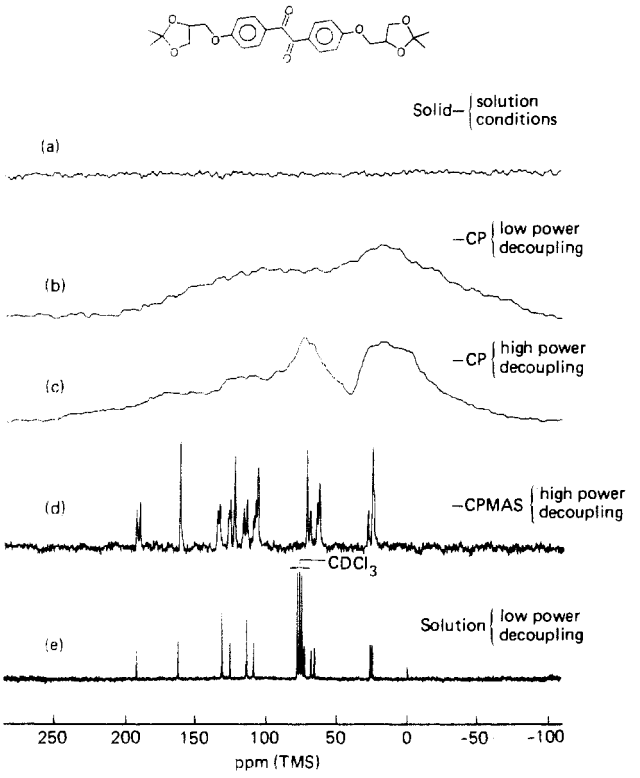

Figure 1. Solid-state ^{13}C NMR spectra (obtained at 15 MHz) of the bisacetonide of 4,4′-bis[(2,3-dihydroxypropyl)oxy]benzil. Experimental conditions: (a) 680 mg, using conventional 60° flip-angle carbon pulses with a 10-s-delay between scans and 6-kHz proton decoupling; (b) same as (a), with proton–carbon cross polarization with a 1-s delay between scans; (c) same as (b), but with 43-kHz proton decoupling; (d) 34 mg with the same parameters as (c) with the addition of magic angle spinning (MAS); (e) 34 mg dissolved in $CDCl_3$, with the same NMR parameters as (a). Total times required for the spectra (4096 scans) were (a and e) 12 h; (b–d) 1.2 h.

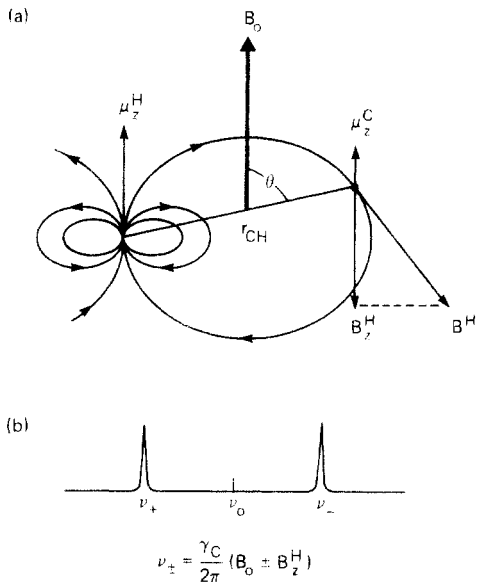

Figure 2. Proton–carbon dipolar coupling in an isolated C–H bond: (a) lines of force from the proton magnetic moment (shown here in the + state, parallel to the external field $\mathbf{B}_0$) generate a static field $\mathbf{B}^H$ at the ^{13}C nucleus. Since $B^H << B_0$, the ^{13}C moment experiences only B_z^H, the component of $\mathbf{B}^H$ which is antiparallel to $\mathbf{B}_0$ for $\theta > 54.7°$ (^{13}C nuclei bonded to protons which are in the - state will experience a field B_z^H parallel to $\mathbf{B}_0$); (b) the resulting ^{13}C spectrum for a sample of isolated C–H fragments with a single orientation (θ).

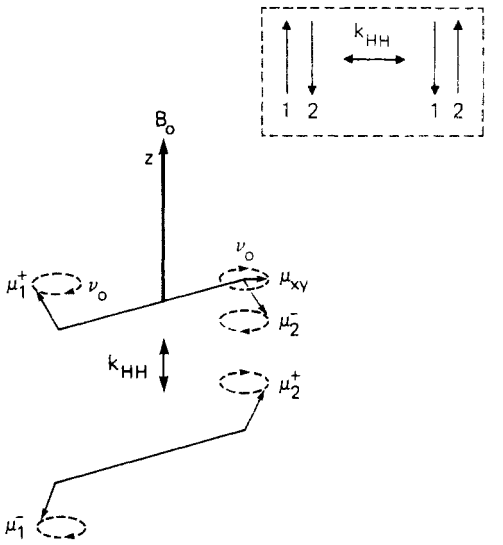

Figure 3. Flip-flop (spin diffusion) process for dipolar coupled protons. The + and – superscripts denote spin state. μ_{xy} is the component of μ_2^- perpendicular to $\mathbf{B}_0$ rotating at ν_0. k_{HH} is the flip-flop rate, and is comparable to the proton line width. A simplified representation of a flip-flop is shown in the inset.

calculated from eq 1. Usually, the ^{13}C resonances in a polycrystalline organic material are broad featureless envelopes of unresolved splittings (Figure 1b) because (1) the ^{13}C nuclei are dipolar coupled to many protons and spectral complexity (i.e., the number of splittings) soars as the number of coupled protons increases, (2) since crystallites in the sample are randomly oriented, all values of θ (and therefore of $\Delta\nu_{CH}$) are equally probable, and (3) the distance to nearby protons may vary for chemically different carbons, again resulting in a distribution of dipolar splittings.[8]

Spin Diffusion among Protons

The large widths that would be calculated by using eq 1 are not usually observed because eq 1 describes coupling between ^{13}C nuclei and "static" proton moments, whereas fluctuations of the proton moments usually reduce this line width. These fluctuations arise from rapid simultaneous transitions ("flip-flops") of dipolar-coupled protons having antiparallel moments.[9] This process, called spin diffusion, is peculiar to coupled nuclei with the same precession frequency and is not meant to imply any physical movement of the nuclei. The dynamics of the flip-flop process (for protons) are shown in Figure 3. The rotating (in the xy plane) component of the spin which is in the higher energy state (μ_2^-), precessing at a frequency ν_0, acts like a resonant rf field at the site of μ_1^+, which is also precessing at ν_0. Thus μ_1^+ absorbs a photon and changes state to μ_1^-, while μ_2^- drops to μ_2^+, emitting a photon of equal energy; this process limits the lifetime of the spin state, leading to uncertainty broadening of the proton resonance. The homogeneous proton line width ($\Delta\nu_{HH}$) is roughly equal to the flip-flop rate (k_{HH}). Values of $\Delta\nu_{HH}$ in organic solids are typically in the 10–50-kHz range. The proton spin state will fluctuate at this rate and

(8) Dipolar interactions among the dilute (1.1%), spatially isolated ^{13}C nuclei are small due to the inverse third power dependence on internuclear distance and will usually be averaged to zero by magic angle spinning.[5]

(9) A. Abragam, "The Principles of Nuclear Magnetism", Oxford University Press, London, 1961, p 98.

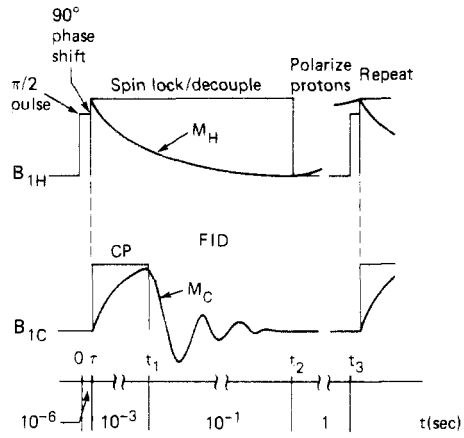

Figure 4. Single-contact spin-lock cross polarization (CP) rf pulse sequence, showing the time dependence of the carbon and proton magnetization. Time scales for various parts of the sequence are shown (in seconds). For CPMAS, the sample is continuously rotated about the magic axis (see Figure 8).

average the ^{13}C–^{1}H interaction to $\Delta\nu_{CH}$ ($\Delta\nu_{CH}/\Delta\nu_{HH}$).[10] Since $\Delta\nu_{HH} > \Delta\nu_{CH}$ for most organic solids, a reduction of the ^{13}C line width is expected. Nonetheless, proton dipolar broadening of several kilohertz is normal, and is removed by a decoupling technique slightly different from that used in solution NMR.

Proton Decoupling by Spin Locking

Proton dipolar broadening in ^{13}C spectra of solids could be removed by a high power version of the decoupling technique used in solution NMR spectroscopy. As shown in Figure 1, however, sensitivity in solid state ^{13}C spectra is significantly enhanced by proton–carbon cross polarization (CP), which is initiated by spin locking the protons (Figure 4).[4,11] Since a spin-locked nucleus is decoupled from other kinds of nuclei,[11] it is most convenient to decouple the protons simply by continuing the spin lock through the time during which the carbon signal (FID) is acquired ($t_1 < t < t_2$; Figure 4). The decoupling dynamics of a spin lock will be covered in this section, which will also serve as the basis for a subsequent discussion of the role of spin locking in the cross polarization process. Spin locking is most easily visualized in the rotating reference frame (Figure 5—the times shown refer to the CP pulse sequence in Figure 4). At resonance, the rotating frame is a coordinate system moving in synchronism with the precession of the proton moments around $\mathbf{B}_0$ at a frequency $\nu_{0H} = (\gamma_H/2\pi)\mathbf{B}_0$. Thus, if only $\mathbf{B}_0$ is present, the spins appear stationary in the rotating frame, meaning that forces due to $\mathbf{B}_0$ are not manifest in this frame, and $\mathbf{B}_0$ can be neglected. If, however, an rf field is applied at ν_{0H}, the rotating component of this field ($\mathbf{B}_{1H}$) moves in synchronism with, and therefore appears stationary in, the rotating frame (Figure 5a). The proton magnetization $\mathbf{M}_{0H}$ will now precess around $\mathbf{B}_{1H}$ at a frequency $\nu_{1H} = (\gamma_H/2\pi)\mathbf{B}_{1H}$. The initial step in the spin lock is a $\pi/2$ pulse (Figure 5a). The phase of the rf field is then electronically shifted by 90°. As shown in Figure 5b, this has the effect, in the rotating frame, of orienting $\mathbf{M}_{0H}$ along $\mathbf{B}_{1H}$. While spin locked, individual proton moments execute a precession about

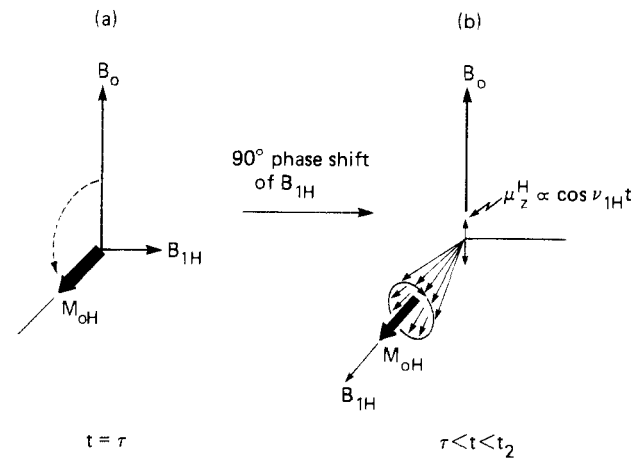

Figure 5. Proton spin locking dynamics viewed in the rotating frame at resonance $\nu_0 = (\gamma/2\pi)B_0$: (a) just after the $\pi/2$ pulse and (b) after the 90° phase shift of the rf field. Precession of individual proton moments around $\mathbf{B}_{1H}$ results in an oscillatory component along the z axis. The times refer to the pulse sequence in Figure 4.

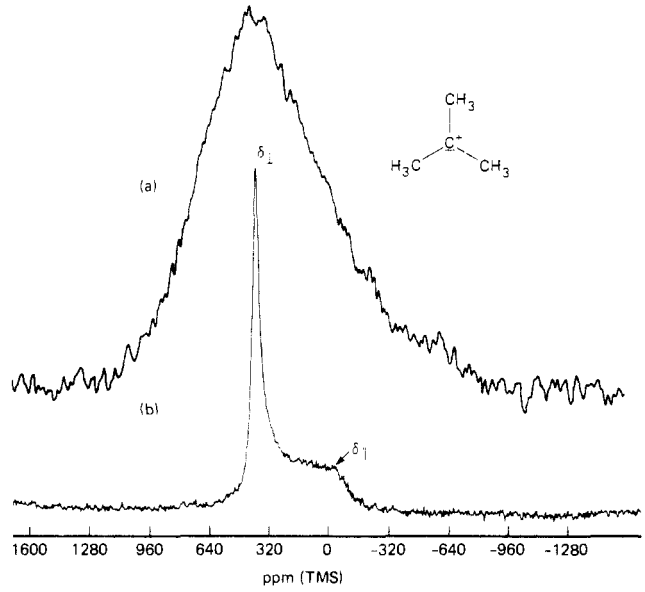

Figure 6. ^{13}C NMR spectra at −180 °C of the *central* carbon of the *tert*-butyl cation prepared from 2-chloro-2-methylpropane-2-^{13}C and SbF_5: (a) without decoupling, and (b) with strong (43 kHz) ^{1}H and ^{19}F decoupling.[13] For the sake of clarity, spectral contribution from the methyl carbons has been subtracted.

$\mathbf{B}_{1H}$, and the z components oscillate at a frequency ν_{1H}. If $\nu_{1H} >> \Delta\nu_{HH}$, a condition for effective decoupling,[10] proton flip-flops will not disrupt this precession, and the ^{13}C spins will experience the field from a coherently averaged z component of the proton moment, $\langle\mu_z^H\rangle$. For sinusoidal variation, $\langle\mu_z^H\rangle = 0$, so that the ^{1}H–^{13}C dipolar coupling (eq 1), and concomitant proton broadening, is removed. To satisfy the requirement that $(\gamma_H/2\pi)B_{1H} > \Delta\nu_{HH}$, spin lock (decoupling) fields of 10 mT (43 kHz) or more are normally used.[12,13] The necessity for such high power decoupling is apparent in Figure 6, which shows the solid-state spectrum of the central carbon of the *tert*-butyl cation, prepared in a

(10) Reference 9, p 571; G. Sinning, M. Mehring, and A. Pines, *Chem. Phys. Lett.*, **43**, 382 (1976).
(11) S. R. Hartmann and E. L. Hahn, *Phys. Rev.*, **128**, 2042 (1962).
(12) Much larger rf fields are required if the broadening nucleus (e.g., ^{19}F) has a large chemical shift anisotropy: W. W. Fleming, C. A. Fyfe, J. R. Lyerla, H. Vanni, and C. S. Yannoni, *Macromolecules*, **13**, 460 (1980).
(13) P. C. Myhre and C. S. Yannoni, *J. Am. Chem. Soc.*, **103**, 230 (1981); C. S. Yannoni, V. Macho, and P. C. Myhre, *ibid.*, **104**, 907 (1982).

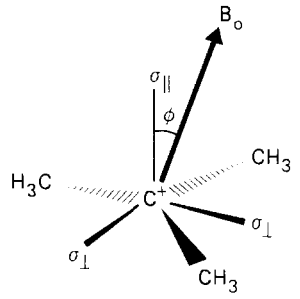

Figure 7. Principal axes ($\sigma_{\parallel}$,$\sigma_{\perp}$) of the chemical shift tensor for the central carbon of the *tert*-butyl cation. The orientation of this axially symmetric tensor is completely defined by ϕ.

SbF_5 matrix.[13] The top spectrum was obtained without decoupling, while the bottom spectrum emerged when 43-kHz decoupling fields for both ^1H and ^{19}F were used.

Relaxation of Spin-Locked Magnetization

Spin-locked magnetization (shown in Figure 5b) represents a quasi-equilibrium state which decays in a time $T_{1\rho}$, the rotating frame relaxation time.[14] The term "lock" is used because $T_{1\rho}$ in solids is usually much longer (it can even be comparable to T_1, the spin–lattice relaxation time) than the short time (T_2) in which magnetization decays when the rf field is turned off. For protons, $T_{2H} \sim \Delta\nu_{HH}^{-1} \sim 10^{-5}$ s, while $T_{1\rho}^{H}$ is generally in the millisecond to second range. The magnitude of $T_{1\rho}$ is not important for decoupling, but, as discussed later, will be a factor in obtaining reliable intensities in CP spectra. Molecular motion with correlation frequencies $\sim(\gamma_H/2\pi)B_{1H}$ (i.e., in the kilohertz range) are effective in destroying spin-locked magnetization. Therefore, $T_{1\rho}$ measurements can be used to probe molecular motions that are orders of magnitude slower than those studied by conventional T_1 measurements.[2,15]

Chemical Shift Anisotropy

Even after dipolar broadening has been removed, ^{13}C spectra of solids will appear much broader than solution spectra of the same material. The spectrum of the central carbon of the *tert*-butyl cation shown in Figure 6b is a dramatic example. The asymmetric lineshape arises because the chemical shift depends on the orientation of molecule-fixed axes with respect to the external field; i.e., the shift is anisotropic.[16] Since all molecular orientations are equally probable in a powder sample, the spectrum obtained, even for a single kind of carbon, is a superposition of these orientation-dependent shifts. The observed shift can be written

$$\delta = (\gamma/2\pi)B_0\sigma_{zz} \tag{2}$$

where σ_{zz} is the magnetic shielding measured along $\mathbf{B}_0$ (Figure 7). σ_{zz} can be related to shielding along orthogonal directions (principal axes) in the molecule by direction cosines:

$$\sigma_{zz} = \sum_{i=1}^{3} \sigma_i \cos^2 \theta_i \tag{3}$$

σ_i is the shielding at the nucleus when $\mathbf{B}_0$ points along the ith principal axis, and θ_i is the angle this axis makes with $\mathbf{B}_0$. Since the central carbon in the *tert*-butyl cation is a site of axial symmetry, $\sigma_1 = \sigma_2 = \sigma_{\perp}$ and $\sigma_3 = \sigma_{\parallel}$. This makes eq 3 particularly simple:

$$\sigma_{zz} = \sigma_{\parallel} \cos^2 \phi + \sigma_{\perp} \sin^2 \phi \tag{4}$$

where ϕ is the angle $\mathbf{B}_0$ makes with the symmetry axis (Figure 7). The spectrum of Figure 6b shows that the shielding of the charged carbon is highly anisotropic since the shift for $\phi = \pi/2$ ($\delta_{\perp}$) is 450 ppm downfield from the shift for $\phi = 0$ ($\delta_{\parallel}$). The difference, $\delta_{\parallel} - \delta_{\perp}$, is called the chemical shift anisotropy (CSA). For nuclei in a site of axial symmetry, the intensity profile of the CSA powder pattern permits unique assignment of spectral extrema to shielding along specific molecular directions.[16] For nuclei in less-than-axial sites, the powder pattern becomes more complex, and assignment of spectral features to molecular directions cannot generally be made without a single crystal study[17a] or two-dimensional NMR experiments.[17b] This is very useful structural information, since the magnitude and direction of the shielding components can give detailed insight into molecular charge distribution.[17c] The CSA shown in Figure 6b reflects the extremely large deshielding effects found in carbonium ions;[18] maximum shift anisotropies for carbons in neutral molecules are generally $\sim$200 ppm.[1b]

Removal of the Chemical Shift Anisotropy by Magic Angle Spinning

Although the solid-state NMR spectrum of a single carbon, like that shown in Figure 6b, can be highly informative, molecules of interest will often have several chemically different carbons, and the CSA powder patterns will probably overlap to give broad spectra as in Figure 1c. Magic angle spinning is the one known method which can be used in solids to remove the chemical shift anisotropy while the isotropic shift observed in solution NMR is retained.[5] The sample is rotated rapidly about an axis which makes an angle of 54.7° with $\mathbf{B}_0$. The effect of this rotation on the CSA can be illustrated for the central carbon of the *tert*-butyl cation. σ_{zz} (eq 4) can be written explicitly in terms of isotropic and anisotropic contributions to the magnetic shielding:

$$\sigma_{zz} = \langle\sigma\rangle + \sigma^a \tag{5}$$

where $\langle\sigma\rangle$ is the isotropic shielding $[^1/_3(\sigma_{\parallel} + 2\sigma_{\perp})]$ observed in solution spectra, and σ^a is the anisotropic part of σ_{zz}:

$$\sigma^a = {}^1/_3(\sigma_{\parallel} - \sigma_{\perp})(3\cos^2\phi - 1) \tag{6}$$

The effect of MAS on the anisotropic shift can be understood from eq 6 by noting that ϕ becomes time dependent upon sample rotation. If the spinning rate, ν_r, is greater than the breadth of the CSA powder pattern, the carbon experiences an average anisotropic shielding, given by

$$\langle\sigma_a(t)\rangle = {}^1/_3(\sigma_{\parallel} - \sigma_{\perp})\langle 3\cos^2\phi(t) - 1\rangle \tag{7}$$

where the angular brackets denote a time average over

(14) A. G. Redfield, *Phys. Rev.*, **98**, 1787 (1955).
(15) T. M. Connor, "NMR, Basic Principles and Progress", Vol. 4, Springer-Verlag, New York, 1971.
(16) U. Haeberlen, "High Resolution NMR in Solids. Selective Averaging", Supplement 1 to *Adv. Magn. Reson.*, Academic Press, New York, 1976, Chapter 3.
(17) (a) S. Pausak, A. Pines, and J. S. Waugh, *J. Chem. Phys.*, **59**, 591 (1973); (b) M. Linder, A. Hohener, and R. R. Ernst, *ibid.*, **73**, 4959 (1980); (c) B. R. Appleman and B. P. Dailey, *Adv. Magn. Reson.*, 7, 231 (1974); K. W. Zilm, R. T. Conlin, D. M. Grant, and J. Michl, *J. Am. Chem. Soc.*, **102**, 6672 (1980); J. B. Grutzner and N. R. Nowicki, *Chem. Rev.*, in press.
(18) G. A. Olah and D. J. Donavan, *J. Am. Chem. Soc.*, **99**, 5026 (1977).

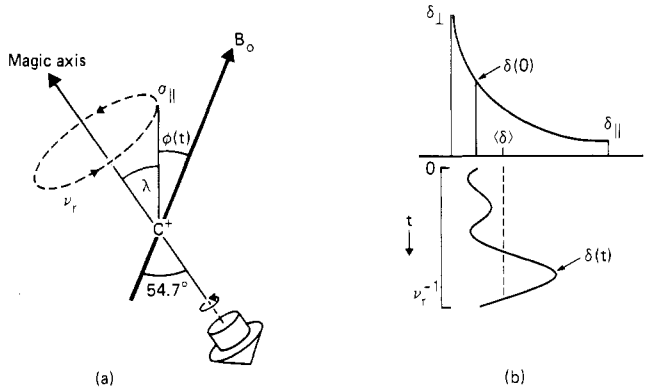

Figure 8. (a) Geometry of the MAS experiment for a *tert*-butyl cation with orientation as in Figure 7, except only the cation symmetry axis ($\sigma_\parallel$) is shown; (b) time dependence of the frequency (shift) $\delta(t)$ for a single cation as the sample is rotated about the magic axis. The average frequency is at the isotropic shift, $\langle\delta\rangle$.

a sample rotation period (ν_r^{-1}). The geometry of the magic angle spinning experiment for a *tert*-butyl cation with the initial orientation (at the start of data acquisition) of Figure 7 is shown in Figure 8a. Only the orientation of the symmetry axis of the cation which, according to eq 4, determines the orientation dependence of the chemical shift completely, is shown. The average in eq 7 can be calculated by using a mathematical identity:[19]

$$\langle 3\cos^2\phi(t) - 1\rangle = \tfrac{1}{2}(3\cos^2\lambda - 1)[3\cos^2(54.7°) - 1] = 0 \quad (8)$$

where λ is the angle between the cation symmetry axis and the sample spinning axis. Now $\cos(54.7°) = 1/3^{1/2}$, so that $\langle\sigma_a(t)\rangle$ vanishes for all values of λ (i.e., for ^{13}C nuclei in all cations). The averaging process described above can also be visualized spectroscopically by following the time dependence of the shift $\delta(t)$ for a cation with a particular initial orientation and shift $\delta(0)$. This is shown schematically in Figure 8b; it is evident that the average frequency over a rotational period indeed lies at the isotropic chemical shift $\langle\delta\rangle = (\gamma/2\pi)B_0\langle\sigma\rangle$. Even though cations with different initial orientations (shifts) have distinct frequency trajectories as the sample rotates, the time-average frequency for all of them is identical. The same holds true for nuclei in nonaxial sites, so that all CSA patterns "magically" collapse to the respective isotropic shifts with this spinning geometry. The ^{13}C spectrum of the solid benzil derivative shown in Figure 1d, obtained by using strong proton decoupling and magic angle spinning, can be compared with the solution NMR spectrum (Figure 1e) of the same material. The remarkable carbon-by-carbon resolution, as well as the similarity to (perhaps even more so the subtle difference from) the solution spectrum, illustrate the potential of this technique for detailed structural and dynamical studies of solids.

Sensitivity Enhancement by Cross Polarization

Since ^{13}C is a low abundance nucleus with a small magnetic moment and long polarization times, sensitivity is always at a premium in ^{13}C NMR spectroscopy. In organic solids, sensitivity is further reduced by broadening due mainly to dipolar coupling with nearby

(19) H. Margenau and G. M. Murphy, "The Mathematics of Physics and Chemistry", Van Nostrand, New York, 1956, p 109.

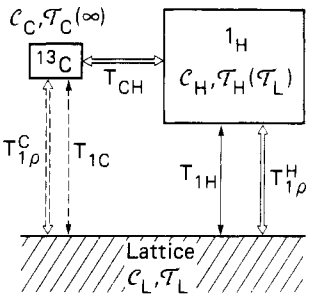

Figure 9. Large ^1H, small ^{13}C, and infinite lattice reservoir, characterized by a heat capacity, C (vide infra), and temperature $\mathcal{T}$. Temperatures in parentheses are those at the start ($t = 0$) of the CP sequence. The $T_{1\rho}^C$ and T_{CH} connections are made during CP time, while $T_{1\rho}^H$ processes are operative during the entire proton spin lock (see Figure 4). Dashed lines signify weak coupling (long relaxation times).

protons (Figure 1a). Ironically, the same ^1H–^{13}C dipolar coupling which is so inimical to resolution in solid-state ^{13}C spectra provides the opportunity for enhancing sensitivity by the cross-polarization (CP) technique,[4] which uses the large proton magnetization to polarize the ^{13}C nuclei.[20] Cross-polarization spectroscopy is a particularly effective version of double resonance in the rotating frame;[11] it is based on the dynamics and thermodynamics of nuclear spin systems.[21] Many CP schemes are possible,[4] but only the commonly used single-contact spin-lock version will be covered in this Account. The pulse sequence is shown in Figure 4 along with a time scale, which will be referred to as the sequence is followed. Since spin thermodynamics is central to any discussion of cross polarization, an introduction to the concept of spin temperature[22] may prove useful, and will be given by following the variation of *proton* spin temperature during the CP sequence shown in Figure 4.

Spin Temperature in Solids. When an organic solid is placed in a magnetic field $\mathbf{B}_0$, individual protons populate Zeeman levels with energies $\pm(\gamma_H/2\pi)B_0/2$, corresponding to spin alignment parallel and antiparallel to $\mathbf{B}_0$. The protons also interact with each other via dipolar coupling and experience the mutual spin flips characteristic of the spin diffusion process (Figure 3). If a *single* proton changes Zeeman levels by exchanging energy with the lattice, this information is transmitted in a short time, typically <100 μs, to a large number of neighboring protons by a propagation of such mutual flips. Thus, the protons will soon (<100 μs) be found in a state of internal equilibrium, which can be considered a single thermodynamic reservoir (Figure 9) characterized by a temperature $\mathcal{T}_H$, with Zeeman levels populated according to a Boltzmann distribution. After several spin lattice relaxation times (T_{1H}), the proton reservoir will come to equilibrium with the lattice, and $\mathcal{T}_H$ will be equal to the lattice temperature $\mathcal{T}_L$. The proton magnetization is then given by a Curie law:[23]

$$M_{0H} = C_H B_0/\mathcal{T}_L \quad (9)$$

C_H is the proton Curie constant: $C_H = N_H\gamma_H^2\hbar^2/4k$.

(20) Magnetization, polarization, and reservoir size (Figure 9) are used interchangeably in this Account.

(21) Readers interested in a more detailed discussion of these topics are referred to C. P. Slichter, "Principles of Magnetic Resonance", Springer-Verlag, Berlin, 1978, Chapters 6 and 7.

(22) Reference 9, Chapter V; A. Abragam and W. G. Proctor, *Phys. Rev.*, **109**, 1441 (1958).

(23) Reference 21, p 191.

N_H is the number of protons and k is the Boltzmann constant. The heat capacity of the corresponding proton reservoir depends, as one might expect, on the number of spins, and is given by $\mathcal{C}_H = N_H\gamma_H^2B_0^2/4$.[24] The first step (after proton polarization) in the CP experiment is a proton spin lock along the rf field (Figure 5). The proton reservoir is perturbed by this sequence, but shortly after the phase shift of the rf field ($t = \tau$, Figures 4 and 5), the protons regain internal equilibrium. The physics of the spin-locked state has been illuminated by Redfield, who made the ingenious argument that this equilibrium should be identified with spin interactions viewed in the rotating reference frame (i.e., without the effect of the external dc magnetic field, $\mathbf{B}_0$), and postulated that the corresponding spin states have energies $\pm(\gamma_H/2\pi)B_{1H}/2$, determined by the strength of the *rf field*.[14] Furthermore, he concluded that the population of these states is given by a Boltzmann distribution characterized by a *spin temperature in the rotating frame*. Under these conditions, the proton magnetization, which is conserved during the spin lock, is given by[4]

$$M_{0H} = C_HB_{1H}/\mathcal{T}_H \qquad (10)$$

$\mathcal{T}_H$ is the proton spin temperature in the rotating frame, which can be calculated by combining eq 9 and 10. Since $B_{1H} \sim 10$ mT while $B_0 \geq 1$ T, this temperature is very low; e.g., for a sample at room temperature, $\mathcal{T}_H \sim 3$ K.[25] The physical reality of this kind of temperature difference between a spin system and the surrounding lattice has been conclusively demonstrated.[22] As discussed earlier in this Account, the rotating-frame reservoir established by a spin-lock sequence is a quasi-equilibrium state,[14] since the proton magnetization decays with a time constant $T_{1\rho}^H$, typically milliseconds. The cross polarization process is now considered in detail.

Cross Polarization. At $t = \tau$ (Figure 4), the carbon magnetization (M_C) is small, since ^{13}C nuclei will generally take much longer than the protons to polarize in $\mathbf{B}_0$ (i.e., $T_{1C} > T_{1H}$). The corresponding ^{13}C spin temperature is given by $\mathcal{T}_C = C_CB_0/M_C$, where C_C is the ^{13}C Curie constant, $N_C\gamma_C^2\hbar^2/4k$. Since M_C is small, $\mathcal{T}_C$ will be large; i.e., the ^{13}C reservoir is "hot". A thermal link between the hot carbon and cooled proton reservoirs (Figure 9) is then established by irradiating the carbons on resonance during the first part of the proton spin lock (CP time, $\tau < t < t_1$) and adjusting rf field amplitudes so that

$$(\gamma_C/2\pi)B_{1C} = \nu_{1C} = \nu_{1H} = (\gamma_H/2\pi)B_{1H} \qquad (11)$$

This is the Hartmann–Hahn matching condition for nuclear double resonance in the rotating frame.[11] As shown in Figure 10, the CP dynamics for an isolated ^1H–^{13}C pair can be understood in terms of oscillating z components of the precessing spins, viewed simultaneously in the carbon and proton rotating frames which have coincident z axes (along $\mathbf{B}_0$).[26] The proton spin-locked moment has a z component (μ_z^H) which oscillates at a frequency ν_{1H} (Figure 5b), thereby producing a dipolar field $B_z^H \cos \gamma_{1H}t$, where B_z^H is given in eq 1.

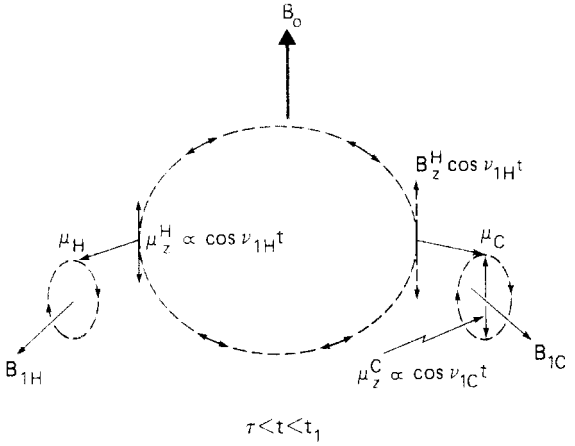

Figure 10. Cross polarization dynamics in the rotating frames at resonance for both nuclei ($\nu_{0C} = (\gamma_C/2\pi)B_0$, $\nu_{0H} = (\gamma_H/2\pi)B_0$). The ^{13}C spin, μ_C, experiences lines of force (dashed) due to an alternating field generated by the spin-locked proton (μ_H). Since $\nu_{1H} = \nu_{1C}$ when the Hartmann–Hahn condition (eq 11) is satisfied, resonant cross relaxation between ^{13}C and ^1H is possible. The time period refers to the pulse sequence in Figure 4.

The ^{13}C moment, precessing about $\mathbf{B}_{1C}$, has a z component oscillating at ν_{1C} and experiences a resonant perturbation from μ_z^H, since $\nu_{1H} = \nu_{1C}$ when eq 11 is satisfied. Thus, the carbon and proton spins, with identical oscillatory components in their respective rotating frames, can cross relax efficiently by the energy-conserving spin flips (Figure 3) normally reserved for identical nuclei. When eq 11 is satisfied, the cross relaxation time, T_{CH}, depends mainly on the strength of the ^1H–^{13}C dipolar coupling, given by eq 1.[27,28] After several T_{CH} (typically 0.5–5.0 ms), the ^1H and ^{13}C spin reservoirs come to equilibrium at a common temperature. This temperature will be close to that of the spin-locked proton magnetization, because the carbon spin reservoir (with a relatively small number of nuclei, i.e., $N_C \sim 10^{-2}N_H$) does not have enough heat capacity to significantly raise the temperature of the proton reservoir. Assuming that there has been no decay of the spin-locked proton magnetization during CP time (i.e., that $T_{1\rho}^H >> T_{CH}$), the proton and, thus, carbon spin temperature at the end of the cross polarization period ($t = t_1$) will be very low: $\mathcal{T}_C = \mathcal{T}_H = \mathcal{T}_L(B_{1H}/B_0) \sim 10^{-3}\mathcal{T}_L$. This reduction of carbon spin temperature translates into a growth, during CP time, of ^{13}C magnetization along the rf field $\mathbf{B}_{1C}$, which can be calculated by using eq 9–11. The result is that the enhanced polarization is $M_C = (\gamma_H/\gamma_C)M_{0C} \approx 4M_{0C}$,[4] where M_{0C} is the polarization which would be generated in $\mathbf{B}_0$ after waiting several T_{1C} (i.e., $M_{0C} = C_CB_0/\mathcal{T}_L$).[29]

(24) M. Goldman, "Spin Temperature and Nuclear Magnetic Resonance in Solids", Oxford University Press, London, 1970, p 22.

(25) If the magnetization were somehow aligned antiparallel to B_{1H}, the spin temperature would be negative, a possibility owing to the upper bound on the energy of nuclear spins in a magnetic field; ref 21, p 199.

(26) F. M. Lurie and C. P. Slichter, *Phys. Rev. A*, **133**, 1108 (1964).

(27) Since the sample is continuously rotated about the magic axis, the ^1H–^{13}C dipolar coupling, which has the same kind of angular dependence as the chemical shift anisotropy, should be averaged to zero if $\nu_r >> \Delta\nu_{CH}$. However, proton spin diffusion limits the lifetime of a carbon coupled to a proton to $\Delta\nu_{HH}^{-1}$ s, which disrupts the coherent averaging of the ^1H–^{13}C dipolar coupling by MAS. Therefore, unless $\nu_r >> \Delta\nu_{HH}$ (and this is rarely the case), ^1H–^{13}C dipolar coupling will survive under MAS conditions. The familiar scalar coupling (J_{CH}) multiplets observed in solution NMR spectra are not affected by MAS (T. Tereo, H. Miura, and A. Saika, *J. Chem. Phys.*, **75**, 1573 (1981), and ref 5c) but are collapsed by the strong proton decoupling.

(28) J. Schaefer, E. O. Stejskal, and R. Buchdahl, *Macromolecules*, **10**, 384 (1977); J. Schaefer and E. O. Stejskal, *Top. Carbon-13 NMR Spectrosc.*, **3**, 283 (1980).

(29) The first high-resolution ^{13}C spectrum in an organic solid was obtained by using a technique[30] which monitors the corresponding *increase* in spin temperature of the *protons* during cross polarization: C. S. Yannoni and H. E. Bleich, *J. Chem. Phys.*, **55**, 5406 (1971).

From here on, the experiment resembles a conventional FT NMR scheme. A carbon free induction decay (FID) follows termination of the carbon pulse and is stored in a computer; during this time ($t_1 < t < t_2$), the protons are decoupled by the spin-lock field. The CP sequence can then be repeated following a proton repolarization period of several $T_{1H}(t_2 < t < t_3)$. Typically $T_{1H} << T_{1C}$, so that in a given time period, many more FID's can be accumulated by using the CP technique than with $\pi/2$ pulses followed by carbon repolarization. After a sufficient number of FIDs have been accumulated, the spectrum is obtained by Fourier transformation. Thus, cross polarization is used to polarize the carbons more quickly (by $\sim T_{1H}/T_{1C}$) and to a greater degree (by ~ 4) than is possible by natural relaxation processes.

This analysis of cross polarization involves several assumptions about experimental conditions, many or all of which can be met depending on the particular sample, temperature, and spectrometer. These include $B_{1C}, B_{1H} >>$ proton and carbon natural line widths, and $T_{1C} > T_{1H} \geq T_{1\rho}{}^{H} >$ CP time $> T_{CH}$. When these conditions cannot be met, optimum sensitivity enhancement is not obtained. Nevertheless, the times required to obtain CPMAS spectra are usually comparable to, and in many cases shorter than, those used to obtain solution ^{13}C spectra (compare Figure 1, d and e). Other things being equal, the best sensitivity in CP spectra is expected from solids with a short T_{1H} and a relatively long $T_{1\rho}{}^{H}$. These conditions are often met in molecules with reorienting methyl groups.[31] Additional time can be saved in CP experiments on samples that contain unpaired electrons[32] or by preserving any proton polarization that remains at the end of the spin lock.[33]

Relative Intensities in CP Spectra

For quantitative work, intensities must be proportional to the number of carbons of a given kind. This requires that carbons which cross polarize slowly be given sufficient time to equilibrate with the spin-locked proton reservoir, which decays in a time $\sim T_{1\rho}{}^{H}$. For reliable relative intensities, $T_{1\rho}{}^{H}$ should therefore be longer than the longest T_{CH}.[34] The CP rate ($T_{CH}{}^{-1}$) can vary widely, especially in molecules containing both protonated and nonprotonated carbons.[28] This becomes evident from a rough calculation of the cross relaxation rate when the matching condition (eq 11) is satisfied:[4,29]

$$T_{CH}{}^{-1} \sim \Delta\nu_{CH}{}^{2}/\Delta\nu_{HH}$$

$\Delta\nu_{CH}$ is given by eq 1, and $\Delta\nu_{HH}$ is the strength of the ^{1}H–^{1}H dipolar coupling. Thus, the CP rate depends on $r_{CH}{}^{-6}$, so that carbons which have no bonded protons will cross polarize more slowly. The disparity in CP rate can also be turned to good use by running experiments as a function of CP time to distinguish between protonated and nonprotonated carbons.[28] Accordingly, T_{CH} plays a role in CP experiments much like that of T_{1C} in conventional pulsed NMR experiments. Another trick that has proved useful for distinguishing protonated from nonprotonated carbons exploits the fact that in the absence of proton decoupling the FID for protonated carbons decays quickly, relative to that from nonprotonated carbons. Therefore, by removing proton decoupling for a short period following CP time a spectrum consisting mainly of peaks from nonprotonated carbons may be obtained.[35]

Elimination of Artifacts by Spin Temperature Inversion

A clever use of the spin temperature concept has significantly reduced instrumental artifacts in the CP experiment.[36] The phase of the $\pi/2$ pulse on the protons is shifted by 180° every other spin-lock sequence, so that $\mathbf{M}_{0H}$ is spin locked alternately parallel and antiparallel to $\mathbf{B}_{1H}$, making the corresponding proton spin temperature ($\mathcal{T}_H$) positive and negative,[25] respectively. Thus, the ^{13}C spin temperature, which follows $\mathcal{T}_H$, is also reversed every CP sequence, i.e., carbon magnetization grows alternately parallel or antiparallel to $\mathbf{B}_{1C}$ in the carbon rotating frame. This shifts the phase of the ^{13}C FID by 180° every CP sequence, even though the carbon rf field itself retains the same phase. By alternately adding and subtracting the ^{13}C FID, rf transients are subtracted out, while the carbon FIDs are coherently added. This has become a standard procedure in CP spectroscopy and is especially useful for minimizing transmitter feedthrough due to long receiver recovery times.

Resolution in the CPMAS Experiment

Technical Limitations. Although the major source of broadening in ^{13}C spectra of solids is proton dipolar coupling, this can be removed by spin locking if $\nu_{1H} >> \Delta\nu_{HH}$.[10] Resolution is also sensitive to the orientation of the spinning axis in the MAS experiment; roughly speaking, this axis must be within 0.5° of the magic angle to reduce a CSA powder pattern to 1% of its static value.[5c] This leaves line widths as large as 2 ppm, which can usually be reduced further by trial-and-error adjustment of the angle. In a certain sense, the spinning speed can also be thought of as a factor in resolution. At high dc field strengths, CSA powder patterns can span 10 kHz or more, and complete MAS averaging requires comparable spinning frequencies, which are difficult to achieve. If the spinning rate is less than the chemical shift anisotropy, the spectrum is broken up into a complex profile of sidebands centered around each isotropic shift.[37] This leads to a loss in sensitivity, as well as confusion in spectral assignment. Despite this complication, techniques which permit recovery of the isotropic (and even anisotropic) shifts from these sidebands have been developed and demonstrated for simple molecules.[37,38] Given the rich content of a spectrum like that of the benzil derivative shown in Figure 1d, however, it is clear that from the viewpoint of the high-resolution spectroscopist, it is preferable to

(30) H. E. Bleich and A. G. Redfield, *J. Chem. Phys.*, **55**, 5405 (1971); **67**, 5040 (1977).
(31) H. W. Bernard, J. E. Tanner, and J. G. Aston, *J. Chem. Phys.*, **50**, 5016 (1969).
(32) R. A. Wind, J. Trommel, and J. Smidt, 22nd Experimental NMR Conference, Asilomar, CA, April 1981; S. Ganapathy, A. Naito, and C. A. McDowell, *J. Am. Chem. Soc.*, **103**, 6011 (1981).
(33) J. Tegenfeldt and U. Haeberlen, *J. Magn. Reson.*, **36**, 453 (1979).
(34) A. N. Garroway, W. B. Moniz and H. A. Resing, *ACS Symp. Ser.*, *No.* **103**, 67 (1979).
(35) S. J. Opella and M. H. Frey, *J. Am. Chem. Soc.*, **101**, 5854 (1979).
(36) E. O. Stejskal and J. Schaefer, *J. Magn. Reson.*, **18**, 560 (1975).
(37) E. Lippmaa, M. Alla, and T. Tuherm, Proceedings of the 19th Congress Ampere, Heidelberg (Groupement Ampere, Heidelberg, 1976), p 113.
(38) M. Maricq and J. S. Waugh, *Chem. Phys. Lett.*, **47**, 327 (1977); J. Herzfeld and A. E. Berger, *J. Chem. Phys.*, **73**, 6021 (1980); W. P. Aue, D. J. Ruben, and R. G. Griffin, *J. Magn. Reson.*, **43**, 472 (1981).

be as close as possible to the fast-spin limit. A method has also been introduced to reduce spectral congestion by eliminating sidebands.[39]

Sample Effects. Even under ideal experimental CPMAS conditions, static and/or dynamic effects can limit resolution in particular samples. Amorphous materials, such as polymers[28] or matrices,[13] may have a distribution of isotropic chemical shifts for a single carbon. This can contribute several parts per million of broadening. Furthermore, interference between coherent motion (e.g., spin locking or sample rotation) and molecular motion can conspire to degrade the resolution gained in the CPMAS technique.[3a,28,40] Splittings due to solid state effects (see Figure 1d) or coupling to nuclei with quadrupole moments (e.g., ^{14}N, ^{35}Cl) may complicate or broaden ^{13}C spectra of solids,[12,41] but can also lead to new structural information.[42] Some of these, as well as other more subtle effects, have been considered in a recent comprehensive study.[43] The authors conclude that the resolution in ^{13}C spectra of organic solids will generally not be as good as in liquids, and furthermore, that increasing the magnetic field may not help.

Conclusions

^{13}C CPMAS spectroscopy in organic solids uses high power decoupling (spin locking) to remove proton dipolar broadening, magic angle spinning to eliminate broadening due to carbon chemical shift anisotropy, and coherently driven proton–carbon cross relaxation to enhance ^{13}C sensitivity. The result is well-resolved ^{13}C NMR spectra of organic solids.

The spectrum of the benzil derivative shown in Figure 1d dramatically illustrates the power of the CPMAS technique for structural studies in solids, purely from the viewpoint of resolution. Another major area that has been opened up through CPMAS is the study of molecular dynamics on a carbon-by-carbon level. Individual carbon T_1[44] or $T_{1\rho}$ measurements have already been used to study main chain and side group dynamics in polymers.[28,45] In this respect, the power of CPMAS is substantially increased by variable temperature capability,[2,46] especially for studies of dynamic processes at temperatures heretofore inaccessible by solution NMR. The following Account will report on the use of a CPMAS spectrometer with variable temperature capability to address a variety of structural and dynamical problems of chemical interest.

(39) W. T. Dixon, *J. Magn. Reson.*, **44**, 220 (1981).
(40) These effects can, however, be used to study molecular motion: D. Suwelack, W. P. Rothwell, and J. S. Waugh, *J. Chem. Phys.*, **73**, 2559 (1980); W. P. Rothwell and J. S. Waugh, *ibid.*, **74**, 2721 (1981).
(41) E. Lippmaa, M. Alla, T. J. Pehk, and G. Engelhardt, *J. Am. Chem. Soc.*, **100**, 1929 (1978).
(42) E. Lippmaa, M. Alla, and E. Kundla, 18th Experimental NMR Conference, Asilomar, CA, April 1977; J. R. Lyerla, C. S. Yannoni, D. Bruck, and C. A. Fyfe, *J. Am. Chem. Soc.*, **101**, 4770 (1979); H. D. W. Hill, A. P. Zens, and J. Jacobus, *ibid.*, **101**, 7090 (1979); J. G. Hexem, M. H. Frey, and S. J. Opella, *ibid.*, **103**, 224 (1981); A. Naito, S. Ganapathy, and C. A. McDowell, *J. Chem. Phys.*, **74**, 5393 (1981); N. Zumbulyadis, P. M. Henrichs, and R. H. Young, *ibid.*, **75**, 1603 (1981).
(43) D. L. VanderHart, W. L. Earl, and A. N. Garroway, *J. Magn. Reson.*, **44**, 361 (1981).
(44) D. A. Torchia, *J. Magn. Reson.*, **30**, 613 (1978).
(45) A. N. Garroway and D. L. VanderHart, *J. Chem. Phys.*, **71**, 2773 (1979); W. S. Veeman and E. M. Menger, *Bull. Magn. Reson.*, **2**, 77 (1981); W. W. Fleming, C. A. Fyfe, R. D. Kendrick, J. R. Lyerla, H. Vanni, and C. S. Yannoni, *ACS Symp. Ser.*, No. 142, 193 (1980).
(46) C. A. Fyfe, H. Mossbrugger, and C. S. Yannoni, *J. Magn. Reson.*, **36**, 61 (1979).

Chemical Applications of Variable-Temperature CPMAS NMR Spectroscopy in Solids

JAMES R. LYERLA* and COSTANTINO S. YANNONI*

IBM Research Laboratory, San Jose, California 95193

COLIN A. FYFE*

Guelph-Waterloo Centre for Graduate Work in Chemistry, University of Guelph, Guelph, Ontario, Canada N1G2W1

Received August 10, 1981 (Revised Manuscript Received April 1, 1982)

Introduction

Significant advances in the development of "high-resolution" nuclear magnetic resonance (NMR) techniques for the characterization of molecular properties of solids have occurred in the past decade.[1] From the viewpoint of chemical applications, the most promising of these developments is the cross-polarization (CP),[2] magic angle spinning (MAS),[3] NMR experiment. Indeed, the intervening 6 years since Schaefer and Stejskal[4] first reported high-resolution ^{13}C spectra of polymers in the glassy state have witnessed the extension of this spectroscopy into a diversity of chemically interesting areas, e.g., natural as well as synthetic

James Lyerla received his B.A. in Chemistry from Southern Illinois University (1966) and his Ph.D. in Physical Chemistry from the University of Utah (1971). After postdoctoral work at the University of Toronto and the National Bureau of Standards, he joined the IBM Research Laboratory at San Jose (1975) where he is currently manager of polymer characterization.

Costantino S. Yannoni attended Harvard College and received his doctorate from Columbia University in 1967. He is currently a Research Staff Member in the Chemical Dynamics Department at the IBM Research Laboratory in San Jose, CA. His research involves application of NMR techniques to the study of molecular structure and dynamics in liquid crystals and solids. He has an abiding interest in the use of NMR to study reactive intermediates.

Colin A. Fyfe is Professor of Chemistry at the University of Guelph. He received both B.Sc. and Ph.D. degrees from the University of St. Andrews, Queen's College, Dundee, Scotland, and spent 2 years as a Killam Fellow at the University of British Columbia. His research interests are in the investigation of reaction mechanisms, detection of transient intermediates by flow NMR, and the investigation of the dynamic structures of solids by high-resolution solid-state NMR. He was recipient of the 1981 Merck, Sharp & Dohme Award in Organic Chemistry.

(1) R. W. Vaughan, *Annu. Rev. Phys. Chem.*, **29**, 397 (1979).
(2) S. R. Hartmann and E. L. Hahn, *Phys. Rev.*, **128**, 2042 (1962); A. Pines, M. G. Gibby, and J. S. Waugh, *J. Chem. Phys.*, **59**, 569 (1973).
(3) (a) E. R. Andrew, *Prog. Nucl. Magn. Reson. Spectrosc.*, **8**, 1 (1971); (b) I. J. Lowe, *Phys. Rev. Lett.*, **2**, 285 (1959). (c) B. Schneider, D. Doskočilová, J. Babka, and Z. Ruzicka, *J. Magn. Reson.*, **37**, 41 (1980).
(4) J. Schaefer, E. O. Stejskal, and R. Buchdahl, *Macromolecules*, **8**, 291 (1975); **10**, 384 (1977).

0001-4842/82/0115-0208$01.25/0